Supplementary Information

Integrating entropy-driven DNA circuit with tetrahedral scaffold as a generic in-situ electrochemical biosensor for amplified detection of microRNAs

Xuyao Wang [a,*], Junlan Zhu [a], Peng Shu [a], Jiajing Wang [b], Maowen Huang [b], Hengchao Chen [c] and Haifen Ma [c]

[a] Precision Medicine Research Center, Beilun District People's Hospital, Zhejiang University School of Medicine First Affiliated Hospital Beilun Branch, Ningbo, 315800, PR China
[b] Department of Clinical Laboratory, Beilun District People's Hospital, Zhejiang University School of Medicine First Affiliated Hospital Beilun Branch, Ningbo, 315800, PR China
[c] Department of Pathology, Beilun District People's Hospital, Zhejiang University School of Medicine First Affiliated Hospital Beilun Branch, Ningbo, 315800, PR China

1. Experimental Section

1.1. Materials and reagents

All chemicals were obtained from commercial sources and used without further purification. Tris(2-carboxyethyl) phosphine hydrochloride (TCEP), diethypyrocarbonate (DEPC), mercaptohexanol (MCH), ethylenediaminetetraacetic acid (EDTA), hexaammineruthenium(III) chloride ($[Ru(NH_3)_6]^{3+}$, RuHex), potassium hexacyanoferrate (II) trihydtate, potassium hexacyanoferrate (III) and streptavidin-peroxidase polymer (avidin-HRP) were purchased from Sigma-Aldrich. Benzo[alpha]pyrene-7,8-diol-9,10-epoxide (B[a]PDE) was purchased from Toronto Research Chemicals.

Avidin-HRP was diluted with 1% BSA (bovine serum albumin, Solarbio) in 1×PBS (absin) and the TMB (3,3',5,5'-tetramethylbenzidine) substrate was purchased from Neogen in the format of a ready-to-use reagent (K-blue low activity substrate, H_2O_2 included). Water used in this work was purified by a Millipore system (resistivity = 18 MΩ*cm) and treated with DEPC. All sequences and the modification were supplied by Sangong and the details were listed in Table S1.

1.2. Instruments and measurements

A typical three-electrode system, including a platinum counter electrode, a reference electrode (Ag/AgCl, 3M KCl) and a gold working electrode was applied on an electrochemical workstation (CHI660E, CH Instruments) in this work. In order to investigate the electrochemical properties of the working electrode, cyclic voltammetry (CV), electrochemical impedance spectroscopy (EIS) and square wave voltammetry (SWV) were carried out with the electrolyte (5 mM $[Fe(CN)_6]^{3-/4-}$). CV was scanned from -0.4V to +0.8V with a rate of 100 mV s^{-1}. EIS was conducted upon the application of 0.213 V biasing potential and 10 mV amplitude in the frequency range of 1 Hz to 100 kHz. The scan range and rate of the SWV were -0.4 to 0.8 V and 25 mV s^{-1}, respectively. The step potential was 4 mV and the frequency was set to 15 Hz. Also, chronocoulometry (CC) was performed in the electrolyte of 10 mM Tris-HCl solutions (PH 7.4) containing 50 μM RuHex, and the potential range was from +0.2V to -0.5V with a pulse period of 250 ms.

In the determination of the final HRP redox reaction, CV was performed in the TMB substrate from 0 to +0.7 V at a scan rate of 100 mV s^{-1}, and chronoamperometric detection was carried out subsequently at 100 mV with the steady state obtained within 100 sec.

1.3. Preparation of EDTC

Firstly, the four thiol-modified (C6 S-S) Tetra-A, B, C, D strands were mixed in TM buffer (20 mM Tris-base and 50 mM $MgCl_2$, PH 8.0) with equal TCEP (30 mM, freshly prepared) to a final concentration of 1 μM. The assistant probes were added together or not according to the different situations. Then the solution was heated to 95℃ for 5 min, and quickly cooled down to 4℃ and incubated until use. The gold electrodes

(Au, 2 mm in diameter, CHI101, CH Instrument) were firstly cleaned according to the reported protocol. After drying with N_2 gas, 3 μL of the as-prepared tetrahedral solution were added to the surface and incubated overnight at room temperature. (Cap the electrodes with plastic electrode caps in order to prevent solutions from drying up).

1.4. The procedure of the EDTC reaction

After overnight incubation, the electrode was washed and dried. Then A3 with target miR-96 was added to the surface and incubated for a specific time at room temperature (approximately 25℃, and the optimized time in this experiment was 30 min). Following this, the electrode was washed and dried again, and Avidin-HRP was added to the surface, followed by incubation for 30 min. Finally, the electrode was washed and immersed in TMB solution for signal detection.

1.5. Cell culture and miRNA extraction

Beas-2B cells from ATCC were maintained at 37℃ in a 5% CO_2 incubator with DMEM supplemented with 10% fetal bovine serum (FBS). After growing to approximate 90% density, cells were treated with B[a]PDE for 12h. Following this, dead cells were washed away with PBS and the remained were continued to be cultured. The procedure of B[a]PDE exposure were repeated for three times and the cells were finally harvested with TRIzol reagents (Invitrogen). Total RNA was extracted by miRNeasy Mini Kit (QIAGEN). And qRT-PCR was performed on a QuantStudio 5 (ABI).

1.6. Experiment process by the microplate reader

In these serial experiments, A2 was labeled with fluorophore FITC at the 3' termini and worked as the final detection medium to present the strength of the fluorescence signal. In Curve a, TDN with abundant TITC-A2 and T-A1 was assembled on 24 individual electrodes overnight. Due to the special washing process in the electrode reactions, unreacted FITC-A2 was flushed away and didn't affect subsequent testing. After washing and drying, target miR-96 and A3 were added to the surface to initiate the EDTC reaction and incubated for series of time (0, 5, 10, 15, 20, 25, 30, 35, 40 min). Every 5 minutes, the drop on the corresponding electrode was gained and transferred to the 384 well standard opaque plate and finally detected together when all the drop was collected. Curve b shared the same process, but replaced the TDN with a single strand Single-A. This strand shared the same sequence with Tetra-A, but lacked the sequence of its tetrahedral scaffold portion. It was thiol modified at the 3' termini and can assembled on the gold electrode surface according to the previous reports. In Curve c, the entire reaction occurred in the liquid phase within the wells of a 384 plate. In order to distinguish the FITC-A2 bound on the strand or not, we designed BHQ-A1 strand. In this substrate (TDN, FITC-A2, BHQ-A1), FITC was quenched, and only when the target miR-96 and A3 were presented, FITC-A2 and BHQ-A1 were replaced and separated, leading to the recovery of fluorescence. The whole process was recorded by a microplate reader in the Kinetic mode and every 5 minutes, the fluorescence was detected.

2. Results and discussion

2.1. The Gibbs Free Energy Equation

The entire entropy-driven process was expressed as a reaction equation in Fig. S1 and the corresponding Gibbs free energy equation was shown as below:

$$\Delta G = \Delta H - T\Delta S \quad (1)$$

ΔH and ΔS were the changes of enthalpy and entropy in the system and T represents the thermodynamic temperature. As the total number of base pairs remained unchanged before and after the reaction, ΔH could be regarded as 0 and the entropic gain of $T\Delta S$ was the driving force. Under non-standard conditions, the equation below was further adopted to estimate the final concentration of reactants and products.

$$\Delta G = \Delta G_F^0 + \Delta G_{A1}^0 + \Delta G_{A2}^0 + (\Delta G_T^0) - \Delta G_S^0 - \Delta G_{A3}^0 - (\Delta G_T^0) + RTlnQ \quad (2)$$

In eq 2, *Q* refers to the reaction quotient and ΔG_X^0 is the standard free energy of species *X* under standard conditions, which herein are represented by the negative value of the free energy of the second structure (ΔG_X, expressed in units of kcal/mol) provided by NUPACK. As the tetrahedral structure remained constant during the process and the free energy of this structure was hard to simulate, ΔG_F^0 and ΔG_S^0 were simplified by Single-A. Thus giving

$$G_F^0 + \Delta G_{A1}^0 + \Delta G_{A2}^0 - \Delta G_S^0 - \Delta G_{A3}^0 = -3.42\ kcal/mol \quad (3)$$

When the reaction reaches equilibrium (ΔG = 0), the *Q* value can be reckoned from eqs 2 and 3 and is approximately equal to 320, which is relatively a large reaction quotient. Besides, *Q* value can be expressed as {([F]/C_0)([A1]/C_0)([A2]/C_0)}/{([S]/C_0)([A3]/C_0)} and C_0 = 1 M. For a system with initial concentrations of S and A3 both *c* and the final concentration of F is *x* (expressed in units same with *c*), we can write the following universal equation:

$$\frac{x^3}{C_0(c-x)^2} = 320 \quad (4)$$

As the *Q* value is relatively large, the value of *x* estimated by the bisection method will asymptotically approach *c*. For example, if the value of *c* is 10 nM, the calculated value of *x* is approximately 9.99994 nM, suggesting that the reaction conversion is sufficient.

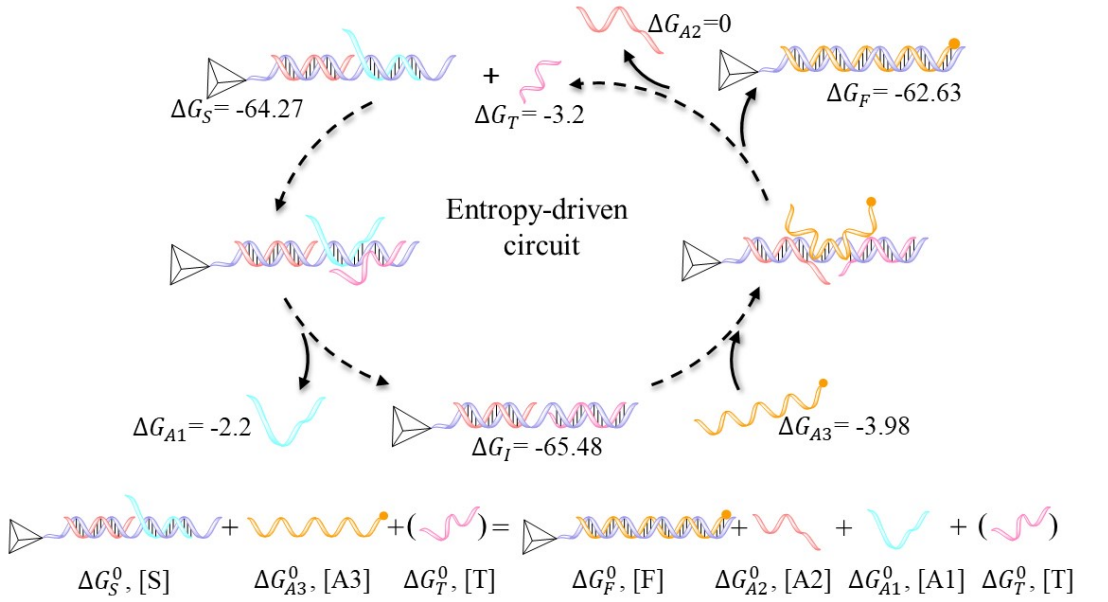

Fig. S1 The entire entropy-driven process expressed as a reaction equation (As the tetrahedral framework remains unchanged during the reaction, only the Tetra-A strand is considered in the free energy calculation).

2.2. PAGE characterization for the Single-A scaffold

Single-A based scaffold and the circuit reaction was also characterized by PAGE. As shown in Fig. S2, similar with the feasibility of the EDTC, this scaffold also facilitates the entropy-driven reaction in the solution.

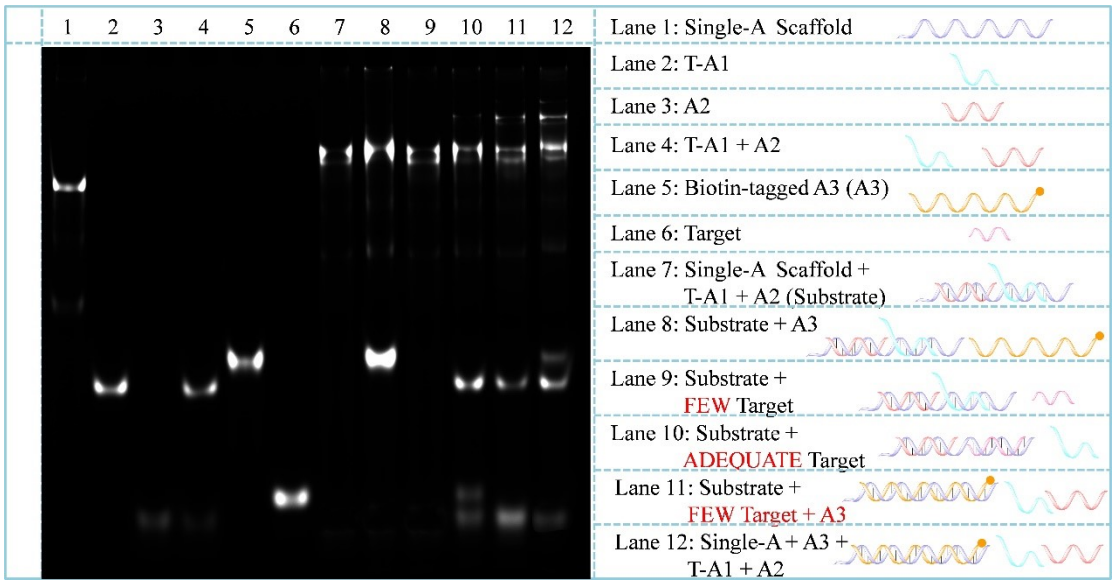

Fig. S2 PAGE characterization (15% native gel) for the feasibility of the Single-A based scaffold and the circuit reaction.

Table S1. DNA and RNA sequences used in this study

Name	Sequence
Tetra-A	AGCAAAAATGTGCTAGTGCCAAAGGGCCGTAAGTTAGTTGGAGATTTTT TACATTCCTAAGTCTGAAACATTACAGCTTGCTACACGAGAAGAGCCGCC
Tetra-B	SH-TATCACCAGGCAGTTGACAGTGTAGCAAGCTG TAATAGATGCGAGGGTCCAATAC
Tetra-C	SH-TCAACTGCCTGGTGATAAAACGACACTACGTG GGAATCTACTATGGCGGCTCTTC
Tetra-D	SH-TTCAGACTTAGGAATGTGCTTCCCACGTAGTGT CGTTTGTATTGGACCCTCGCAT
A1	CCCTTTGGCACTAGCACATT
T-A1	TTTTTTTTTTTTTTTCCCTTTGGCACTAGCACATT
BHQ-A1	BHQ1-CCCTTTGGCACTAGCACATT
A2	TCTCCAACTAACTTACGG
FITC-A2	TCTCCAACTAACTTACGG-FITC
A3	TCTCCAACTAACTTACGGCCCTTTGGCACTAGCACATT-Biotin
Single-A	AGCAAAAATGTGCTAGTGCCAAAGGGCCGTAAGTTAGTTGGAGATTTTT T-SH
miR-96	UUUGGCACUAGCACAUUUUUGCU
miR-137	UUAUUGCUUAAGAAUACGCGUAG
miR-4510	UGAGGGAGUAGGAUGUAUGGUU
miR-615	GGGGGUCCCCGGUGCUCGGAUC
miR-182	UUUGGCAAUGGUAGAACUCACACU
One Mis	UUUGGCACUAGCACAUUUUUACU
Two Mis	UUUGGCACUAGCACAUUAUUACU

Table S2. Comparison of the proposed method with the reported miRNA detection methods.

Method	**Target**	**Linear range**	**LOD**	**Ref.**
Fluorescent	miR-27a	100 pM – 2.5 nM	0.8 pM	1
Fluorescent	Let-7a	25 pM – 250 nM	25 pM	2
Fluorescent	miR-21	100 fM – 2 nM	70 fM	3
Electrochemi-luminescence (ECL)	miR-133a	1 fM – 1 nM	0.33 fM	4
ECL	miR-21	1 fM – 100 pM	0.65 fM	5
Photoelectro-chemical (PEC)	miR-196a	10 aM – 10 pM	3.1 aM	6
PEC	miR-141	1 fM – 10 pM	0.5 fM	7
PEC	miR-21	10 fM – 100 nM	1.5 fM	8
PEC	miR-155	10 aM – 10 pM	3.2 aM	9
Electrochemical	miR-122	0.1 fM – 0.1 μM	53 aM	10
Electrochemical	miR-21	10 fM – 1 nM	2.54 fM	11
Electrochemical	miR-21	1 fM – 10 nM	13.3 aM	12
Electrochemical	miR-31	1 fM – 1 nM	0.31 fM	13

Electrochemical	miR-96	100 aM- 100 pM	74 aM	This

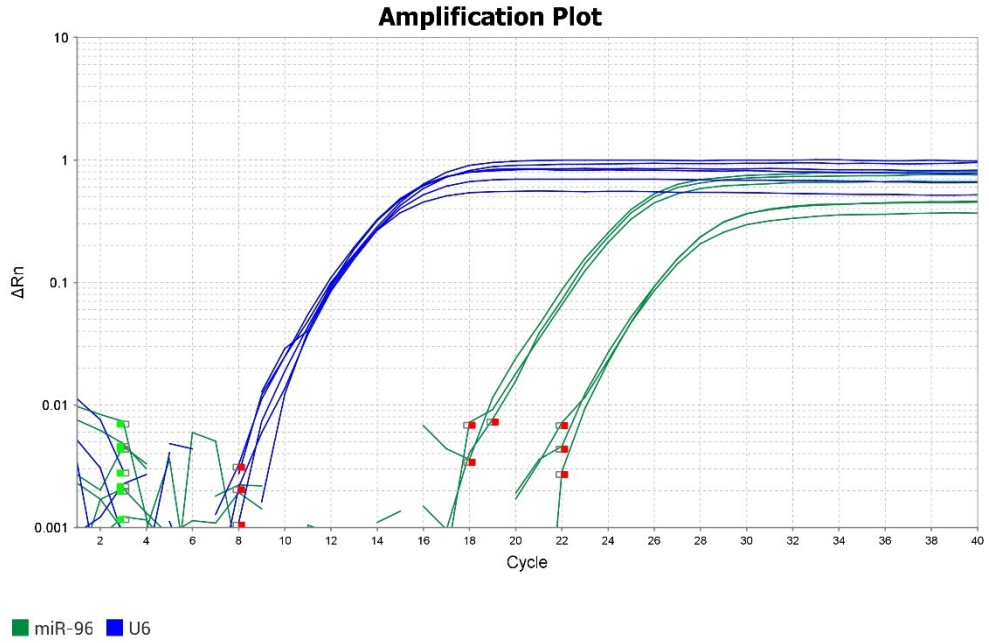

Fig. S4 qRT-PCR curves of the miRNA from Beas-2B cells and B[a]PDE treated Beas-2B cells.

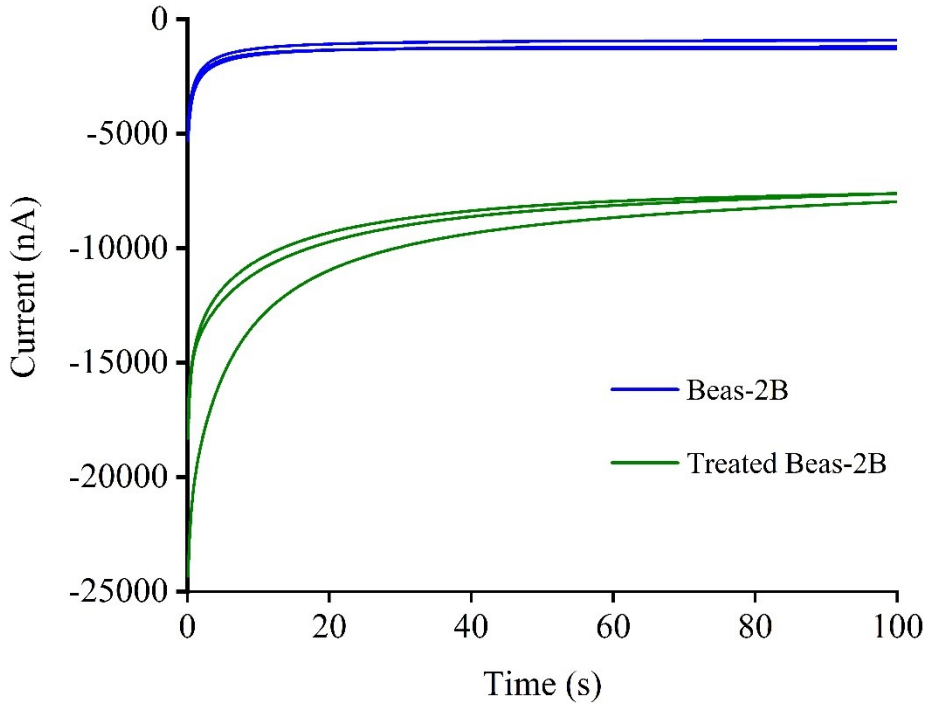

Fig. S5 Current values of the miRNA from Beas-2B cells and B[a]PDE treated Beas-2B cells.

References

1 D. Zhu, B. Lu, Y. Zhu, Z. Ma, Y. Wei, S. Su, L. Wang, S. Song, Y. Zhu and L. Wang, *ACS Appl. Mater. Interfaces*, 2019, **11**, 11220-11226.

2 L. Nie, X. Zeng, L. Hongbo, S. Wang, Z. Lu and R. Yu, *Anal. Chim. Acta*, 2023, **1269**, 341392.

3 Z. Fan, X. Zhao, Y. Dong, J. Zhou, Y. Li, J. Wang, Y. Qi, C. Tan, H. Yu and J. Li, *Int. J. Biol. Macromol.*, 2022, **223**, 931-938.

4 L. Yu, L. Zhu, M. Yan, S. Feng, J. Huang and X. Yang, *Anal. Chem.*, 2021, **93**, 11809-11815.

5 Y. Zhang, G. Xu, G. Lian, F. Luo, Q. Xie, Z. Lin and G. Chen, *Biosens. Bioelectron.*, 2020, **147**, 111789.

6 M. Li, J. Cheng, Z. Yuan, H. Zhou, L. Zhang, Y. Dai, Q. Shen and Q. Fan, *Sensor. Actuat. B-Chem.*, 2021, **345**, 130348.

7 N. Zhang, X.-M. Shi, H.-Q. Guo, X.-Z. Zhao, W.-W. Zhao, J.-J. Xu and H.-Y. Chen, *Anal. Chem.*, 2018, **90**, 11892-11898.

8 L. Zhang, Z. Zhang, R. Liu, S. Wang, L. Li, P. Zhao, Y. Wang, S. Ge and J. Yu, *Sensor. Actuat. B-Chem.*, 2023, **394**, 134334.

9 Y. Chen, L. Xu, Q. Xu, Y. Wu, J. Li and H. Li, *Biosens. Bioelectron.*, 2022, **215**, 114569.

10 Q. Guo, Y. Yu, H. Zhang, C. Cai and Q. Shen, *Anal. Chem.*, 2020, **92**, 5302-5310.

11 Z. Jiang and Z. Liu, *Anal. Biochem.*, 2024, 115593.

12 H. Yang, Q. Dong, D. Xu, X. Feng, P. He, W. Song and H. Zhou, *Anal. Chim. Acta*, 2023, **1283**, 341978.

13 H. Wang, Y. L. Li, Y. J. Fan, J. X. Dong, X. Ren, H. Ma, D. Wu, Z. F. Gao, Q. Wei and F. Xia, *Anal. Chem.*, 2023, **95**, 13659-13667.